

Article

# Effect of Addition of Colloidal Silica to Films of Polyimide, Polyvinylpyridine, Polystyrene, and Polymethylmethacrylate Nano-Composites

Soliman Abdalla <sup>1,\*</sup>, Fahad Al-Marzouki <sup>1</sup>, Abdullah Obaid <sup>2,†</sup> and Salah Gamal <sup>1</sup>

<sup>1</sup> Department of Physics, Faculty of Science, King Abdulaziz University Jeddah, P.O. Box 80203, Jeddah 21589, Saudi Arabia; fmpy@kau.edu.sa (F.A.-M.); sgamal@kau.edu.sa (S.G.)

<sup>2</sup> Department of physical chemistry, Faculty of Science, King Abdulaziz University Jeddah, P.O. Box 80203, Jeddah 21589, Saudi Arabia; aobaid@kau.edu.sa

\* Correspondence: smabdullah@kau.edu.sa; Tel.: +966-582-343-822

† These authors contributed equally to this work.

Academic Editor: Sofoklis Makridis

Received: 4 November 2015; Accepted: 2 February 2016; Published: 6 February 2016

**Abstract:** Nano-composite films have been the subject of extensive work for developing the energy-storage efficiency of electrostatic capacitors. Factors such as polymer purity, nanoparticle size, and film morphology drastically affect the electrostatic efficiency of the dielectric material that forms the insulating film between the conductive electrodes of a capacitor. This in turn affects the energy storage performance of the capacitor. In the present work, we have studied the dielectric properties of four highly pure amorphous polymer films: polymethyl methacrylate (PMMA), polystyrene, polyimide and poly-4-vinylpyridine. Comparison between the dielectric properties of these polymers has revealed that the higher breakdown performance is a character of polyimide (PI) and PMMA. Also, our experimental data shows that adding colloidal silica to PMMA and PI leads to a net decrease in the dielectric properties compared to the pure polymer.

**Keywords:** dielectric break down; polymers; nano-composite; colloidal silica

## 1. Introduction

High operating voltages are an essential characteristic to assess and to improve the efficiency of the energy storage of materials. The dielectric properties of insulating materials separating the electrodes of a capacitor control the maximum electrostatic power of a capacitor. As an example, polypropylene (biaxial-oriented) has a high electrical breakdown that reaches about  $6 \times 10^8$  voltages per meter; however, it has limited energy storage, which reaches about 2 Joules/cm<sup>3</sup>. A solution to improve the energy storage efficiency is to add nano-composite polymers [1–4]. The morphology of the fillers at nano-scale reduces heterogeneities in nano-composites and thus improves the dielectric properties and avoids failure. In addition, to increase these properties, several authors have suggested the addition of metal-oxide nanoparticles TiO<sub>2</sub> and BaTiO<sub>3</sub> [5–10]. In fact, the dielectric properties are very sensitive to the addition of these nanoparticles because the energy density has quadratic dependence on the electric field intensity. Monotonic reduction of the electrical breakdown appears by increasing the metal-oxide nanoparticles [11–17]. This can be analyzed considering randomly dispersed nanoparticles which form percolation networks which can prematurely break down the material, in particular at the high loading rates of TiO<sub>2</sub> and BaTiO<sub>3</sub>. At such rates, it is not a facile task to achieve homogeneous dispersions, but it is more likely to see the formation of the agglomeration which can behave as a defect site, leading to a greater reduction of dielectric properties. Published studies [18–21] have revealed that localized electric fields are created within the matrix with field exclusion. For example, the addition of

(5%–10% v/v) BaTiO<sub>3</sub> nanoparticles generates local electrical fields which negatively affect dielectric properties [20,21]. So, material morphology and individual field contributions are substantial factors that affect dielectric strength and electrical breakdown. Here, the nature of filler materials can decrease field exclusion and gives deeper insight into the effect of morphology on electrical breakdown values. As an example for this effect, the addition of 5% w/w silica nanoparticles increases the electrical breakdown from  $2.69 \times 10^8$  volts/m up to  $3.14 \times 10^8$  volts/m [22,23] and the addition of 1% silica to polypropylene increases the electrical breakdown from  $5.11 \times 10^8$  volts/m up to  $7.78 \times 10^8$  volts/m [24]. In addition, the size of the filler strongly affects the breakdown values [25–27] and the increase of these values can occur with more homogenization of the local electric field distribution through the material [28,29]. However, other authors have proposed that the rise of the breakdown values is essentially due to the presence of some internal barriers through the material which can be reduced by good control of the film morphology. If one forces the electrical field to pass through more curved paths, prolonged breakdown will be produced through tightly structured films [30]. From the experimental point of view, alternating nano-layers of high dielectric polymers poly (vinylidene fluoride) (PVDF) and polycarbonate has increased dielectric strength, which is created by the barriers present in the polymer. These barriers in turn impede the transfer of the electric field [31–34]. Moreover, polyvinyl butyral (PVB) which is added to organically modified montmorillonite (OMMT) in nano-laminar structures has increased the breakdown strength from  $1 \times 10^8$  volts/m (pure film) up to  $1.3 \times 10^8$  volts/m [35,36] when adding 10% v/v OMMT. Also, if the filler substance adopts long-range alignment, breakdown through OMMT-polyethylene nano-composites will increase. For these films, breakdown strength increases from  $2.9 \times 10^8$  volts/m (pure film) up to  $3.7 \times 10^8$  volts/m [36] when adding 6% w/w OMMT. Thus, in general, filler composition, morphology and size are essential factors to get a preferment dielectric material and to better understand these factors at nano-scale composites, and we get a direct comparison between four polymers: polymethyl methacrylate (PMMA), polystyrene (PS), polyimide (PI), and poly-4-vinylpyridine (P4VP) with about half content (50% v/v) colloidal silica. Our data show that the electrical breakdown values through pure PMMA and pure PI are strongly reduced by adding even small quantities of highly dispersed colloidal silica (1% v/v). On the other hand, electrical breakdown values through nano-composites with low dielectric strength such as PS and P4VP increase with colloidal silica added up to 15% v/v. In brief, cheap polymer nano-composites can easily develop amorphous polymers with low breakdown values, especially if there are additional properties as flammability suppression and heat deflection.

## 2. Experimental

Silica nano-composite films have been prepared using the same technique as described elsewhere [37–39] with chemicals from Sigma-Aldrich (St. Louis, MO, USA): 1-poly methyl methacrylate (PMMA), 2-methyl ethylketone (MEK), 3-Celite, 4-methanol, 5-polystyrene, 6-poly-4-vinylpyridine (P4VP), 7-polyimide PI derived from pyromellitic dianhydride/oxidianiline PMDA/ODA. The obtained colloidal silica particles have radius about 15 nm with dispersion into the polystyrene and polyimide host matrices. Phenyl group density has been estimated using exclusion-chromatography techniques and the colloidal silica has been treated with a phenyltrimethoxysilane to ensure homogenous dispersion through the polystyrene. If the dispersion finds a column, the unattached capping agents move through the column after the capped silica. Ultra-violet measurements have been used in order to estimate the relative quantities of attached and unattached capping agents of the eluent which has been compared to initial quantity of capping agent in the reaction to estimate graft density. The hydroxyl area of the uncapped silica has been effectively used with the P4VP and PMMA [40]. For about three days, the colloidal silica dispersion in di-methyl-formamide has been mixed with 10 wt. % polymer solution in di-methyl-formamide which finally gives films about 7 micrometers thick. Using 500 nm film of aluminum as a counter-electrical contact, one ensures the building of a capacitor structure which gives total thickness of about 7  $\mu$ m. The electric breakdown (EBD) and the dielectric characterization have been carried out using power supply ensuring about  $10^4$  volts which is combined with timing circuit that creates

300 volts per second. Thus, the EBD time is about 20 seconds which is in harmony with previously published data [40]. The polymer nano-composite film has been kept in direct contact with a small copper hemispherical-ends-bar to give a direct electrical contact with an effective contact area about  $0.1 \text{ cm}^2$ . This makes good electrical contact and ensures removing the film heterogeneity due to initial manufacturing by local electric fields. The heads of bars are polished after each 15 EBDs. These 15 trails have been carried out for each film to calculate the most probable value of the particle size using Weibull distributions. To get continuous calibrated measurements, one has periodically used free-standing Oriented PolyPropylene (BOPP) film to play the role of test-standard. Spellman generator with  $10^4$  volts, Keithly 6517B and 1260A Solatron have been used to perform the electrical features of the composites. The time duration for each sweep has been kept at 30 seconds and measurements are made at room temperature. The temperature variations at EBD due to Joule heating have been neglected. The measured leakage currents have been taken at half of the critical voltage of EBD.

### 3. Results and Discussion

At  $10^5$  Hz, the above-mentioned nano-polymers have nearly the same dielectric constant; however, they markedly differ in the EBD voltages, which ranged from  $4 \times 10^8$  volts/m for PS to  $8 \times 10^8$  volts/m for PMMA. This shows how much polymer-colloid interactions are crucial for altering the EBD values. The continuous accumulation of nanoparticles is markedly embedded when using polar non-aqueous solvents (e.g., dimethyl formamide (DMF) and dimethylacetamide (DMAC)) when preparing the nano-film [41], which enables the creation of electric charge stabilization of physical properties of colloidal silica. To get an efficient drying rate, the polymer films have been subjected to a  $100^\circ\text{C}$  hot glass plate which also resulted in the aggregation of nanoparticles. More time permits the solvent to evaporate so that the stability of the electrical charges on the colloidal silica is highly reduced and the matrix viscosity becomes strong enough to resist diffusion of particles which leads to a strong dispersion of Polymer Nano Composites (PNCs).

It is noted that this approach gives “qualitatively” similar particles of silica for all the composites, even with high silica content (about 15% v/v) (see Figure 1). At  $10^5$  Hz, the real and imaginary parts of the complex permittivity ( $\epsilon^* = \epsilon' + i\epsilon''$ ; with  $i = \sqrt{-1}$ ) are plotted as a function of silica concentration (Figure 2); in Figure 2a, this is the dielectric constant. The dielectric constant  $\epsilon'$  is plotted as a function of silica concentration, and in Figure 2b, the electrical conductivity  $\sigma$  is plotted as a function of silica concentration. Pure (0% v/v) films have the following dielectric constant: 2.6 for PS, 2.8 for PMMA, 2.9 for PI and 3.3 for P4VP, and these are in fair accordance with a previously published study [42].

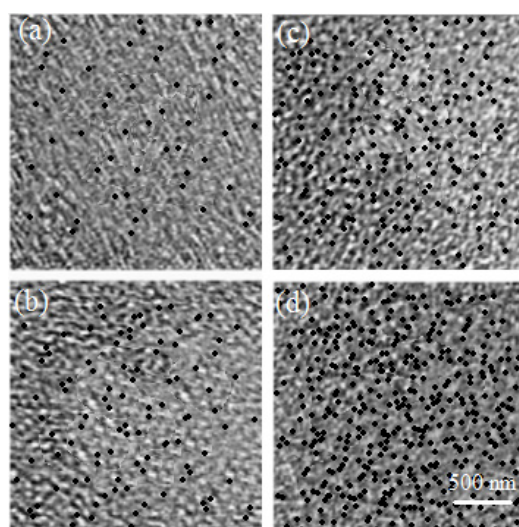


**Figure 1.** TEM illustrations of polymer nano-composite polystyrene films at different silica loading: (a) 1%; (b) 5%; (c) 7.5%; and (d) 15%.

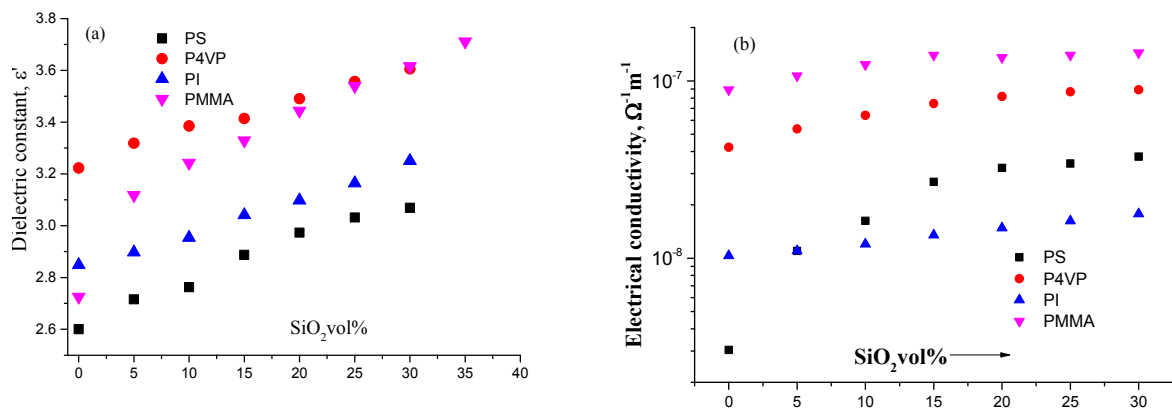


**Figure 2.** (a) The dielectric constant  $\epsilon'$  as a function of silica content for PS, P4VP, PI and PMMA; (b) The electrical conductivity  $\sigma$  as a function of silica content for PS, P4VP, PI and PMMA.

Figure 2a shows the relative dielectric constant  $\epsilon'$  of pure silica as a function of the applied frequency. This figure reveals that silica has a high dielectric function. The dielectric constant of the presented films is illustrated in Figure 2a as a function of the  $\text{SiO}_2$  content. From this Figure, one can see that the  $\epsilon'$  of the films rises linearly with the silica concentration for all films. The dielectric dipoles within polymers are permanently polarized under the application of the DC electric field. However, under the application of the AC field, charges will oscillate following the field depending on the structure and morphology of the polymers, which can be either polar (such as PMMA, PVC, nylon) or non-polar (such as Polytetrafluoroethylene, polyethylene, and polypropylene). At low frequencies, the dipoles on the polymer have sufficient time to align with the applied AC field, though not at high frequencies. So, polar polymers have, in general, their dielectric constant in the range of  $3\epsilon^* < \epsilon' < 9\epsilon^*$  at about 50 Hz and  $3\epsilon^* < \epsilon' < 5\epsilon^*$  at about 100 Hz. This is in good accordance with our findings.

The electrical conductivity  $\sigma$  of the composites is illustrated as a function of the silica concentration at a representative frequency of 100 kHz (Figure 2). The composites' electrical failure as a function of the critical electrical breakdown is illustrated in Figure 3 for different silica concentrations where the cumulative probability function  $P(E)$  for electrical failure is given as [43]:  $P(E) = 1 - \exp[-(E/EBD)^b]$ ; EBD is experimentally reported and taken as a fitting parameter and  $b$  is the shape parameter [44] combined with the linear fit of the probability distribution.

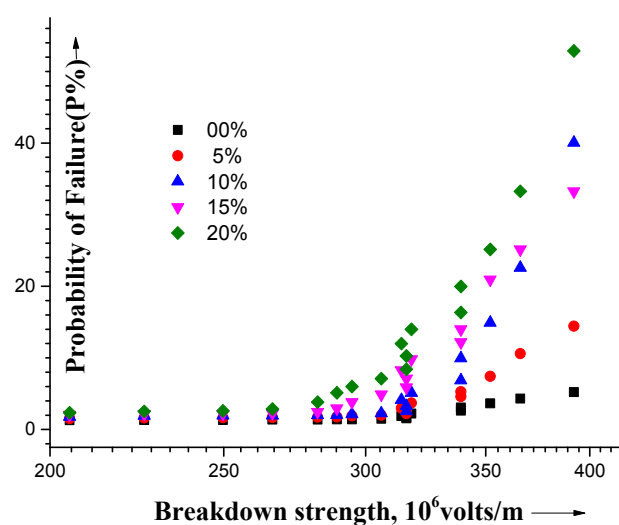


**Figure 3.** The probability of failure (P%) as a function of silica content for PS, P4VP, PI and PMMA.

Figure 4 reveals that the experimental EBD of the composites is sensitive to the chemical properties of the polymer matrix. In particular, PMMA has the most important effect where, if small quantities of PMMA are embedded in silica, it will reduce the EBD by a ratio of about 30%: for example, the EBD of a neat composite is  $8 \times 10^8$  volts/m and it is reduced down to  $3.5 \times 10^8$  volts/m by adding 15% v/v; another example for PI reduces the EBD from  $5.6 \times 10^8$  volts/m (neat value) down to  $4.6 \times 10^8$  volts/m (20%).

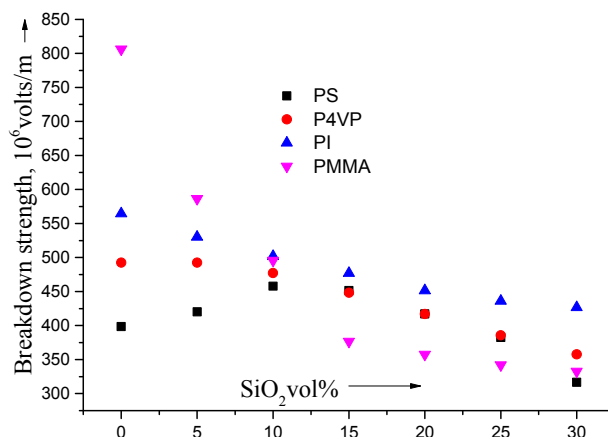


**Figure 4.** The breakdown strength (EBD) as a function of silica content for PS, P4VP, PI and PMMA.

Less important ratios are for P4VP are where the EBD is reduced from  $4.8 \times 10^8$  volts/m down to  $4.4 \times 10^8$  volts/m (10%) when adding 15% v/v. However, for PS, the EBD is increased from  $3.9 \times 10^8$  volts/m (neat) up to  $4.0 \times 10^8$  volts/m (5%). It is noted that all composites suffer a high field leakage current with increasing silica volume fraction. Because PMMA and P4VP have silica with nearly the same hydroxyl exterior, their breakdown behavior [45] is widely different, which reflects the minor effect of the silica surface in the explanation of the experimental data. However, several authors have used the silica surface to improve the breakdown properties with nano-composite films but they have attributed the results to the general morphology of films [45]. Thus, this explains why the addition of minor concentrations of silica at the nano-scale to dielectric films with relatively high breakdown values reduces their dielectric strength. On the contrary, adding silica to the two nano-composite films, P4VP and PI which have relatively weaker breakdown values have a poor effect on the breakdown strength. Giving an electrical analysis which demonstrates the EBD behavior in these dielectric films is not a simple issue and opens the doors to several views. Here, we will focus our scope on only two probable explanations: First, EBD starts initially by the silica colloid nanoparticles. This is logical because failure converges towards nearly the same EBD values for all the dielectric films with increasing silica concentrations. If breakdown only occurs in silica at certain electric fields, this would restrain the dielectric power in PMMA and PI dielectric films. Also, the breakdown value of neat PMMA and PI is higher than the inherent silica breakdown intensity, which is about  $4.5 \times 10^8$  volts/m. However, this last value is little bit higher than the breakdown intensity of PS with its amorphous nature. In fact, it is indistinct why there is a feeble breakdown of PS. The alteration of some tiny fraction of material having stronger inherent failure properties is a potential reason for this weak value of polystyrene (PS). This is because the failure starts from some sensitive imperfections that are sometimes become majority through the polystyrene (PS) matrix [46]. This would implicate that the initiation processes is a less favored mechanism than the effect of silica propagation on failure. Thus, the well-dispersed silica acts as positive factor for forestalling propagations and, at the same time, it can play a negative role for inducing failure, and thus the performance factor depends on the “relative” breakdown rather than the intrinsic properties of the silica itself or its surface. In general, all these electrical breakdown intensities are in harmony with the published data [47]. The term “relative”

breakdown has been used with the restriction that to any critical breakdown failure the positive and negative contradiction roles of silica can happen.

The term “relative” breakdown has been used with the restriction that to any critical relative breakdown? This can be attributed to the “relative” polarity of silica to the polymer matrix. Our experimental data show that the poorer polar film (PS) attains the least breakdown power while the stronger polar film (PMMA) acquires the most elevated breakdown power. So, the addition of silica to crystallite structure formation should have a less significant impact and the same is also said for the role of crystallite in dielectric failure. Films such as bio-oriented polypropylene (BOPP) with non-polar nano-composites have, in general, relatively low breakdown strength, and their execution is controlled essentially by their morphological structure rather than by the polarity of highly disordered regions (amorphous tiny areas). In fact, the insertion of some polar organic groups such as ketones (C=O) increases the polarity of non-polar polymers such as BOPP [46] and this means that the polar organic group plays the role of active trapping sites which introduces the role of scattering centers [47]. The scattering mechanism occurs at the polar surface of silica, leading to more constant trapping centers through the matrix, and improves the electrical breakdown. This happens if one adds silica to a non-polar polymer (for example, low-density polyethylene, polystyrene, BOPP). If the polarity of the silica surface (either native or modified) is stronger than that of the matrix, the propagation of the breakdown to stronger fields will be inhibited. However, conversely, PMMA and most highly polar polymers have the polar surface of silica (either native or modified) which is characterized by less stable trapping centers than inherent to the polymer. Here silica plays the role of a defect that fails at the feeble electric field compared to the surrounding matrix which supplies a lesser quantity of electric power alternative to the superior characteristics of the polar part through the polymer structure. Also, when the volume fractions become sufficiently high, the silica surface area will play the main role of controlling the mechanism of breakdown and, thus, the nanocomposites will be independent of the matrix. In fact, our experimental data show that this happens at a rate of loading of about 15% v/v which is near the critical values previously obtained for spheres in three dimensions [48]. This is well matched with the data in Figure 5 where the Weibull factor  $\beta$  (which depends on the polarity strength) is a function of the silica concentration in the matrix.

One can see that  $\beta$  increases as a reflection of the increasing silica content in polar polymers which also attenuate the dielectric properties of the films. It is worth noting that homogenous trapping sites will be created when uniform distribution of silica colloids occurs through the nanocomposite materials. Also, due to the uniform distribution of silica, the failure variability is reduced in addition to the decrease of the breakdown, which has some important industrial applications. By getting rid of the potential failure at low fields, the design will be controlled by the onset failure field. As an example, the critical electric limit can be highly increased by reducing the film thickness and *vice versa*. For weak silica loading (no more than 10% v/v), PS has lower values of the Weibull factor and thus shows more tendencies for increasing failure variability. One can attribute the electrical breakdown and the dielectric behaviors to the presence of a large number of scattering centers within the polymer matrix which are created from the presence of many particles and structural defects in this matrix. Also, these behaviors are attributed to the presence of nanoparticles which can change the morphology and thus reduce the mobility of the charge carriers. However, the crystallization effects are not, in themselves, essential factors in controlling the dielectric behavior in such materials. In fact, the size of the defects and their effect on the polymer morphology can play a major role either in the polymer bulk or at the surface regions. The size distribution is correlated with the beta-parameter as illustrated in Figure 5. So, we can consider that silica plays the role of a trapping site and not a failure site, which means that the essential role exists on the encountering surface with a probability of a failure event on the particle.

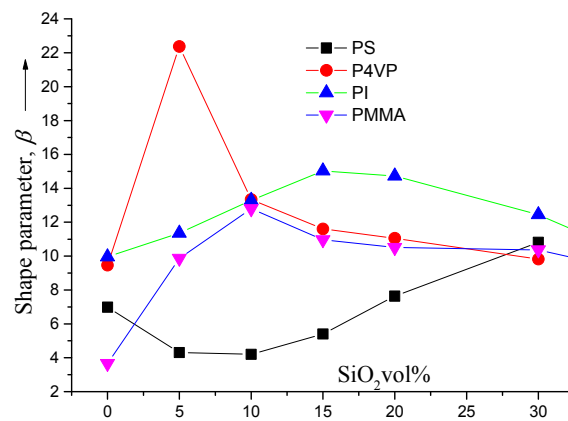


**Figure 5.** The shape parameter ( $\beta$ ) as a function of silica content for PS, P4VP, PI and PMMA.

However, this effect should be minor at low silica concentrations but increase with loading. In PS, this is clearly seen in the general trending of the Weibull factor with more silica loading. Overall, for a strong loading rate of silica (more than 15%), all nano-composites have a tendency to fail with comparable variability and silica masks the host matrix dielectric characteristics and breakdown features.

#### 4. Conclusions

In order to get more efficient materials for energy storage, scientists have developed the abilities of electrostatic capacitors. In particular, electrical breakdown actions are controlled by several competing factors such as agglomeration, substance morphology, and field exclusion. So, one can investigate the essential mechanism(s) for breakdown in dielectric films. When adding colloidal silica to polymethyl methacrylate (or any higher-breakdown amorphous polymers), the critical electrical breakdown will be reduced. However, low-breakdown-strength amorphous polymers such as polystyrene keep high values of breakdown when adding 5%–15% v/v silica. The correlation between matrix and filler will be more important and clearer when taking these remarks into account. The four “clean” samples have revealed excellent dielectric behavior after loading with more than 15% v/v silica with electrical breakdown in the range of more than  $4 \times 10^8$  volts/m but less than  $8 \times 10^8$  volts/m. This proves clearly that the addition of silica to amorphous polymers makes them have the same strong dielectric behavior as the best dielectrics. In fact, silica helps the charge present in the host and nanoparticles to be either scattered or trapped. This stimulates the dielectric properties of polymers and strengthens the storage energy characteristics of these amorphous materials. Also, silica has a weaker failure mode that makes it have a substantial effect in strengthening breakdown. The faint distribution of failure probability for dielectric polymers is to weaken their dielectric power. This is attributed to the strong distribution of crystalline defects throughout the amorphous material. One can correlate the relative polarity of the nanoparticle surface to the matrix with keeping dispersion to arrive at the conclusion that it is necessary to control the polarity of nanoparticles not only to control their morphology and surface. Additional studies are necessary to further explore the basic understandings of the starting and continuing processes in nano-composite materials and to distinguish their particle composition, morphology, and relative polarity influences. However, this general conclusion which is derived from the simple comparison of experimental data of P4VP, PI, PMMA and PS cannot be generalized without taking into account simultaneous studies to examine the chemical composition, source, physical surface and chemical properties on nanoparticles in a wide range of polymer matrices. The data presented in this work stands with what we have previously published [49]: that one of the most important candidates of the next generation of electronics is molecular electronics, as the miniaturization of silicon semiconductors reaches its physical and economic bounds.

**Acknowledgments:** This project was supported by the King Abdulaziz City of Science and Technology general, general direction of research grants—Project No. (1435-35-143), the authors also, acknowledge with thanks the Deanship of Scientific Research, King Abdulaziz University for technical support.

**Author Contributions:** Fahad Al-Marzouki and Salah Gamal conceived and designed the experiments; Salah Gamal performed the experiments; Soliman Abdalla and Abdullah Obaid analyzed the data; Fahad Al-Marzouki contributed reagents/materials/analysis tools; Soliman Abdalla wrote the paper.

**Conflicts of Interest:** The authors declare no conflict of interest.

## References

1. Riggs, B.C.; Elupula, R.; Grayson, S.M.; Chrisey, D.B. Polymer nano composites for energy storage applications. *J. Mater. Chem. A* **2015**, *2*, 3853–3863.
2. Riggs, B.C.; Elupula, R.; Rehm, C.; Adireddy, S.; Grayson, S.M.; Chrisey, D.B. Click-in ferroelectric nanoparticles for dielectric storage. *ACS Appl. Mater. Interfaces* **2015**, *7*, 17819–17825. [[CrossRef](#)] [[PubMed](#)]
3. Ejaz, M.; Puli, V.S.; Elupula, R.; Adireddy, S.; Riggs, B.C.; Chrisey, D.B.; Grayson, S.M. Core-shell structured poly(glycidyl methacrylates)/BaTiO<sub>3</sub> nano composites prepared by surface-initiated atom transfer radical polymerization: A novel material for high energy density dielectric storage. *J. Polym. Sci. A Polym. Chem.* **2015**, *53*, 719–728. [[CrossRef](#)]
4. Riggs, B.C.; Adireddy, S.; Rehm, C.H.; Puli, V.S.; Elupula, R.; Chrisey, D.B. Polymer nano composites for energy storage applications. In Proceedings of ASME 2010 Conference on Smart Materials, Adaptive Structures and Intelligent Systems, Philadelphia, PA, USA, 28 September–1 October 2010; pp. 245–249.
5. Sánchez, F.A.; Redondo, M.; González-Benito, J. Influence of BaTiO<sub>3</sub> submicrometric particles on the structure, morphology, and crystallization behavior of poly(vinylidene fluoride). *Appl. Polym. Sci.* **2014**, *132*. [[CrossRef](#)]
6. Shen, Y.; Hu, Y.; Chen, W.; Wang, J.; Guan, Y.; Du, J.; Zhang, X.; Ma, J.; Li, M.; Lin, Y.; *et al.* Modulation of topological structure induces ultrahigh energy density of graphene/Ba<sub>0.6</sub>Sr<sub>0.4</sub>TiO<sub>3</sub> nanofiber/polymer nano composites. *Nano Energy* **2015**, *18*, 176–186. [[CrossRef](#)]
7. Wang, S.; Huang, X.; Wang, G.; Wang, Y.; He, J.; Jiang, P. Increasing energy efficiency and breakdown strength of high-energy-density polymer nano-composites by engineering the Ba<sub>0.7</sub>Sr<sub>0.3</sub>TiO<sub>3</sub> nano-wire surface via reversible addition fragmentation chain transfer polymerization. *J. Phys. Chem. C* **2015**, *119*, 25307–25318. [[CrossRef](#)]
8. Chen, Z.; Xie, L.; Huang, X.; Li, S.; Jiang, P. Achieving large dielectric property improvement in polymer/carbon nanotube composites by engineering the nanotube surface via atom transfer radical polymerization. *Carbon* **2015**, *95*, 895–903. [[CrossRef](#)]
9. Huang, X.; Jiang, P. Core-shell structured high-*k* polymer nano composites for energy storage and dielectric applications. *Adv. Mater.* **2015**, *27*, 546–554. [[CrossRef](#)] [[PubMed](#)]
10. Feng, Y.; Li, W.L.; Wang, J.P.; Yin, J.H.; Fei, W.D. Core-shell structured BaTiO<sub>3</sub>@carbon hybrid particles for polymer composites with enhanced dielectric performance. *J. Mater. Chem. A* **2015**, *3*, 20313–20321. [[CrossRef](#)]
11. Inui, T.; Koga, H.; Nogi, M.; Komoda, N.; Suganuma, K. A miniaturized flexible antenna printed on a high dielectric constant nanopaper composite. *Adv. Mater.* **2015**, *27*, 1112–1116. [[CrossRef](#)] [[PubMed](#)]
12. Fan, B.; Bai, J. Composites of hybrids BaTiO<sub>3</sub>/carbon nanotubes/polyvinylidene fluoride with high dielectric properties. *J. Phys. D Appl. Phys.* **2015**, *48*, 455303. [[CrossRef](#)]
13. Chen, T.; Qiu, J.; Zhu, K.; Wang, J.; Li, J. Copper phthalocyanine oligomer noncovalent functionalized graphene-polyurethane dielectric elastomer composites for flexible micro-actuator. *Soft Mater.* **2015**, *13*, 210–218. [[CrossRef](#)]
14. Ren, L.; Meng, X.; Zha, J.; Dang, Z. Coulomb block effect inducing distinctive dielectric properties in electroless plated barium titanate@silver/poly (vinylidene fluoride) nano-composites. *RSC Adv.* **2015**, *5*, 65167–65174. [[CrossRef](#)]
15. Chen, M.; Yin, J.; Jin, R.; Yao, L.; Su, B.; Lei, Q. Dielectric and mechanical properties and thermal stability of polyimide-graphene oxide composite films. *Thin Solid Films* **2015**, *584*, 232–237. [[CrossRef](#)]
16. Anjana, J.; Prashanth, K.J.; Asheesh, K.S.; Arpit, J.; Rashmi, P.N. Dielectric and piezoelectric properties of PVDF/PZT composites: A review. *Polym. Eng. Sci.* **2015**, *55*, 1589–1616.



17. Dang, Z.; Lin, Y.; Xu, H.; Shi, C.; Li, S.; Bai, J.; Tang, H.; Lin, Y.; Sodano, H.A. Synthesis of high aspect ratio BaTiO<sub>3</sub> nano-wires for high energy density nano-composite capacitors, fabrication and dielectric characterization of advanced BaTiO<sub>3</sub>/Polyimide nano-composite films with high thermal stability. *Adv. Funct. Mater.* **2008**, *18*, 1509–1517. [[CrossRef](#)]
18. Zhang, G.; Liao, Q.; Zhang, Z.; Liang, Q.; Zhao, Y.; Zheng, X.; Zhang, Y. Novel piezoelectric paper based flexible nanogenerators composed of BaTiO<sub>3</sub> nanoparticles and bacterial cellulose. *Adv. Sci.* **2015**. [[CrossRef](#)]
19. Gonzalez-Benito, J.; Martinez-Tarifa, J.; Sepúlveda-García, M.E.; Portillo, R.A.; Gonzalez-Gaitano, G. Polymer testing, composites based on HDPE filled with BaTiO<sub>3</sub> submicrometric. *Polym. Test.* **2013**, *32*, 1342–1349. [[CrossRef](#)]
20. Olmos, D.; Montero, F.; González-Gaitano, G.; González-Benito, J. Structure and morphology of composites based on polyvinylidene fluoride filled with BaTiO<sub>3</sub> submicrometer particles: Effect of processing and filler content. *Polym. Compos.* **2013**, *34*, 2094–2104. [[CrossRef](#)]
21. Jeong, C.K.; Lee, J.; Han, S.; Ryu, J.; Hwang, J.T.; Park, D.Y.; Park, J.H.; Lee, S.S.; Byun, M.; Ko, S.H.; et al. A Hyper-Stretchable Elastic-Composite Energy Harvester. *Adv. Mater.* **2015**, *27*, 2866. [[CrossRef](#)] [[PubMed](#)]
22. Deka, B.K.; Maji, T.K. Effect of silica nanopowder on the properties of wood flour/polymer composite. *Polym. Eng. Sci.* **2012**, *52*, 1516–1523. [[CrossRef](#)]
23. Al-Sagheer, F.; Ali, A.A.M.; Muslim, S.; Ahmad, Z. Thermal and mechanical properties of chemically bonded aramid-silica nano-composites. *Sci. Technol. Adv. Mater.* **2006**, *7*, 111–118. [[CrossRef](#)]
24. Zua, L.; Li, R.; Jin, L.; Lian, H.; Liu, Y.; Cui, X. Preparation and characterization of polypropylene/silica composite particle with interpenetrating network via hot emulsion sol-gel approach. *Prog. Nat. Sci. Mater. Int.* **2014**, *24*, 42–49. [[CrossRef](#)]
25. Roy, M.; Nelson, J.K.; MacCrone, R.K.; Schadler, L.S. Polymer nano-composite dielectrics: The role of the interface. *IEEE Trans. Dielectr. Electr. Insul.* **2005**, *12*, 629–643. [[CrossRef](#)]
26. Roy, M.; Nelson, J.K.; Crone, R.K.M.; Schadler, L.S. Candidate mechanisms controlling the electrical characteristics of silica/XLPE nano dielectrics. *J. Mater. Sci.* **2007**, *42*, 3789–3799. [[CrossRef](#)]
27. Guo, M.; Fréchet, M.; David, É.; Demarquette, N.R. Polyethylene-based dielectric composites containing polyhedral oligomeric silsesquioxanes obtained by ball milling. *Trans. Electr. Electron. Mater.* **2015**, *16*, 53–61. [[CrossRef](#)]
28. Lewis, T.J. Interfaces and nanodielectrics are synonymous. In Proceedings of the 2004 IEEE International Conferences on Solid Dielectrics, ICSD 2004, Toulouse, France, 5–9 July 2004; pp. 792–795.
29. Tanaka, T. Dielectric nano composites with insulating properties. *IEEE Trans. Dielectr. Electr. Insul.* **2005**, *12*, 914–928. [[CrossRef](#)]
30. Mohanty, A.; Srivastava, V.K. Dielectric breakdown performance of alumina/epoxy resin nano composites under high voltage application. *Mater. Des.* **2013**, *47*, 711–716. [[CrossRef](#)]
31. Rytöluoto, I.; Lahti, K.; Karttunen, M.; Koponen, M. Large-area dielectric breakdown performance of polymer films—Part I: Measurement method evaluation and statistical considerations on area-dependence. *IEEE Trans. Dielectr. Electr. Insul.* **2015**, *22*, 689–700. [[CrossRef](#)]
32. Mackey, M.; Flandin, L.; Hiltner, A.; Baer, E. Confined crystallization of PVDF and a PVDF-TFE copolymer in nano layered films. *J. Phys. D Appl. Phys.* **2011**, *49*, 1750–1761.
33. Mackey, M.; Schuele, D.; Zhu, L.; Baer, E. Reduction of dielectric hysteresis in multilayered films via nanoconfinement. *Macromolecules* **2012**, *45*, 1954–1962. [[CrossRef](#)]
34. Tseng, J.; Tang, S.; Zhou, Z.; Zhu, L. Interfacial polarization and layer thickness effect on electrical insulation in multilayered polysulfone/poly(vinylidene fluoride) films. *Polymer* **2013**, *55*, 8–14. [[CrossRef](#)]
35. Fillery, S.P.; Koerner, H.; Drummy, L.; Dunkerley, E.; Durstock, M.F.; Schmidt, D.F.; Vaia, R.A. Nanolaminates: Increasing dielectric breakdown strength of composites. *ACS Appl. Mater. Interfaces* **2012**, *4*, 1388–1396. [[CrossRef](#)] [[PubMed](#)]
36. Grabowski, C.A.; Koerner, H.; Meth, J.S.; Dang, A.; Hui, C.M.; Matyjaszewski, K.; Bockstaller, M.R.; Durstock, M.F.; Vaia, R.A. Performance of dielectric Nano composites: Matrix-free, hairy nanoparticle assemblies and amorphous polymer-nanoparticle blends. *ACS Appl. Mater. Interfaces* **2014**, *6*, 21500–21509. [[CrossRef](#)] [[PubMed](#)]
37. Oberdisse, J.; Demé, B. Structure of latex-silica nano-composite films: A small-angle neutron scattering study. *Macromolecules* **2002**, *35*, 4397–4405. [[CrossRef](#)]

38. Ma, J.; Xu, Q.; Zhou, J.; Zhang, J.; Zhang, L.; Tang, H.; Chen, L. Synthesis and biological response of casein-based silica nano-composite film for drug delivery system. *Colloids Surf. B Biointerfaces* **2013**, *111*, 257–263. [[CrossRef](#)] [[PubMed](#)]
39. *Standard Test Method for Dielectric Breakdown Voltage and Dielectric Strength of Solid Electrical Insulating Materials at Commercial Power Frequencies*; ASTM D149; ASTM International: West Conshohocken, PA, USA, 2013.
40. Kamel, S. Nanotechnology and its applications in lingo cellulosic, composites, a mini review. *EXPRESS Polym. Lett.* **2007**, *1*, 546–575. [[CrossRef](#)]
41. Peng, R.; Wang, Y.; Tang, W.; Yang, Y.; Xie, X. Progress in Imidazolium ionic liquids assisted fabrication of carbon nanotube and graphene polymer composites. *Polymers* **2013**, *5*, 847–872. [[CrossRef](#)]
42. Fréchet, M. Sur la loi de probabilité de l'écart maximum. *Annales de la Société Polonaise de Mathématique* **1927**, *6*, 93–116.
43. Wang, Y.; Li, J.; Deng, Y. Enhanced ferroelectricity and energy storage in poly(vinylidene fluoride)-clay nano-composite films via nanofiller surface charge modulation. *RSC Adv.* **2015**, *5*, 85884–85888. [[CrossRef](#)]
44. Hahn, J. Fundamentals of nanoscale polymer-protein interactions and potential contributions to solid-state nanobioarrays. *Langmuir* **2014**, *30*, 9891–9904. [[CrossRef](#)] [[PubMed](#)]
45. Duan, C.; Wang, W.; Duan, Q.X.C. Review article: Fabrication of nanofluidic devices. *Biomicrofluidics* **2013**, *7*, 026501. [[CrossRef](#)] [[PubMed](#)]
46. Takala, M.; Ranta, H.; Nevalainen, P.; Pakonen, P.; Pelto, J.; Karttunen, M.; Virtanen, S.; Koivu, V.; Pettersson, M.; Sonnerud, B.; *et al.* Dielectric properties and partial discharge endurance of polypropylene-silica nano-composite. *IEEE Trans. Dielectr. Electr. Insul.* **2010**, *17*, 1259–1267. [[CrossRef](#)]
47. Peter, B.; Shiva, B.; Yogesh, A.; Loye, H. Polymer composite and nano-composite dielectric materials for pulse power energy storage. *Materials* **2009**, *2*, 1697–1733.
48. Yang, M.H.; Hong, S.B.; Choi, B.G. Hierarchical core/shell structure of MnO<sub>2</sub>@polyaniline composites grown on carbon fiber paper for application in pseudo capacitors. *Phys. Chem. Chem. Phys.* **2015**, *17*, 29874–29879. [[CrossRef](#)] [[PubMed](#)]
49. Abdalla, S. Editorial, electric breakdown through nano dielectric films. *J. Mater. Sci. Eng.* **2012**, *1*. [[CrossRef](#)]



© 2016 by the authors; licensee MDPI, Basel, Switzerland. This article is an open access article distributed under the terms and conditions of the Creative Commons by Attribution (CC-BY) license (<http://creativecommons.org/licenses/by/4.0/>).